

# Mountain Home Geothermal Area: Natural State Model

Sabodh K. Garg<sup>1</sup>, Erika Gasperikova<sup>2</sup>, John Shervais<sup>3</sup>, Dennis L. Nielson<sup>4</sup>

<sup>1</sup> Leidos Inc., San Diego, CA

<sup>2</sup> Lawrence Berkeley National Laboratory, Berkeley, CA

<sup>3</sup> Utah State University, Logan, UT

<sup>4</sup> DOSECC Exploration Services LLC, Salt Lake City, UT

## Keywords

*Mountain Home, Snake River Plain, Play Fairway, Natural State, Thermal Modeling, Magnetotellurics*

## ABSTRACT

The Mountain Home area is characterized by high heat flow and temperature gradient. Drilling and temperature data are available from two deep wells (MH-1 and MH-2). Recently, high resolution gravity, ground magnetic, magnetotelluric (MT), and seismic reflection surveys have been carried out in the area in order to define key structural features responsible for promoting permeability and fluid flow. Of particular relevance is the MT survey performed in the area that forms the basis of the 3-D numerical natural state model presented in this paper. The model volume is 2750 cubic kilometers (25 km in the east-west direction, 20 km in the north-south direction, and 5.5 km in the vertical direction). Available temperature profiles from wells MH-1 and MH-2 display good agreement with the computed results.

## 1. Introduction

Under a co-operative agreement with the U.S. Department of Energy (DOE), Utah State University is carrying out a research program to identify promising geothermal prospects in the Snake River Plain (SRP) volcanic province (Shervais et al., 2016, 2017). The goals of this study are to: (1) adapt the methodology of *Play Fairway Analysis* for geothermal exploration, creating a formal basis for its application to geothermal systems, (2) assemble relevant data for the SRP volcanic province from publicly available and private sources, and (3) build a geothermal play fairway model for the SRP that will allow the delineation of the most promising plays. The model will serve to integrate diverse data sets and serve as a point of departure for future exploration efforts in the region. A promising play type is associated with the SRP basaltic sill-

complexes characterized by fault-controlled permeability, volcanic sill heat source, and lake sediment seal (Nielson and Shervais, 2014). The area around Mountain Home Air Force Base in western Snake River Plain hosts a geothermal system of this type.

The Mountain Home area is characterized by high heat flow and temperature gradient. The average temperature gradient exceeds  $80^{\circ}\text{C}/\text{km}$ . Garg et al. (2016) presented a preliminary regional (110 km east-west x 80 km south-north) 3-D numerical model of the natural-state; the model was conditioned using temperature data from five deep holes. Recently, high resolution gravity, ground magnetic, magnetotelluric (MT), and seismic reflection surveys have been carried out in the area surrounding the Mountain Home Air Force Base (MHAFB) in order to define key structural features responsible for promoting permeability and fluid flow (Glen et al., 2017). Of particular relevance is the MT survey (see Figure 1 for MT station locations) that was performed to delineate regions of enhanced permeability and seals.



**Figure 1: Mountain Home area showing the locations of boreholes MH-1 and MH-2 (red circles) and MT stations (white rectangles). The blue line (indicated by white arrows) passing to the south of MH-1 and MH-2 denotes a deep gravity fault. The NW (Lat: 43.1240, Long: -116.0780), NE (43.1211, -115.7707), SW (42.9439, -116.0807), and SE (42.9411, -115.7743) denote the four corners of the area (25 km by 20 km) used for the numerical model described below.**

A 2D regional MT profile (SW-NE) across the SW basin boundary was  $\sim 20$  km long, and resulting 2D resistivity model clearly identified this regional boundary by change from high to low resistivity. Results from 3D resistivity model (Figure 2a) were used to characterize a region  $\sim 13 \times 10$  km in the vicinity of MH-2 well within the basin. Note, due to a high cultural noise at the MHAFB MT data at a few stations were not usable for interpretation and excluded from the 3D MT inversion (e.g., SE and E of the MH-2 well -between MHE1 and MHE3 and MHE1 and

MH04). Low resistivity (1-10 Ohm-m) distribution in 3D resistivity cube outlines the lateral and depth extent of lake beds (and possible alteration zones) that we have proposed is a seal for a potential geothermal reservoir... The uppermost resistive layer (200-500 Ohm-m) is representative of near surface unaltered porous basalts, while increased resistivity (>40 Ohm-m) underneath the low resistivity structure is representative of volcanic formations that could be associated with production of geothermal fluids (Nielson and Shervais, 2014). Figure 2b shows SW-NE resistivity cross-section extracted from 3D resistivity model with a gravity inversion model superimposed in black. The gravity profile is 3 km to SE and runs parallel to this profile (Glen et al., 2017). There is a very good agreement between resistivity and gravity interpretation. Similar structures were recovered on the eastern side of the basin, close to Bostic 1A well, using MT data collected in 1980 by Unocal. Again, MT and gravity interpretations agree well at that location.

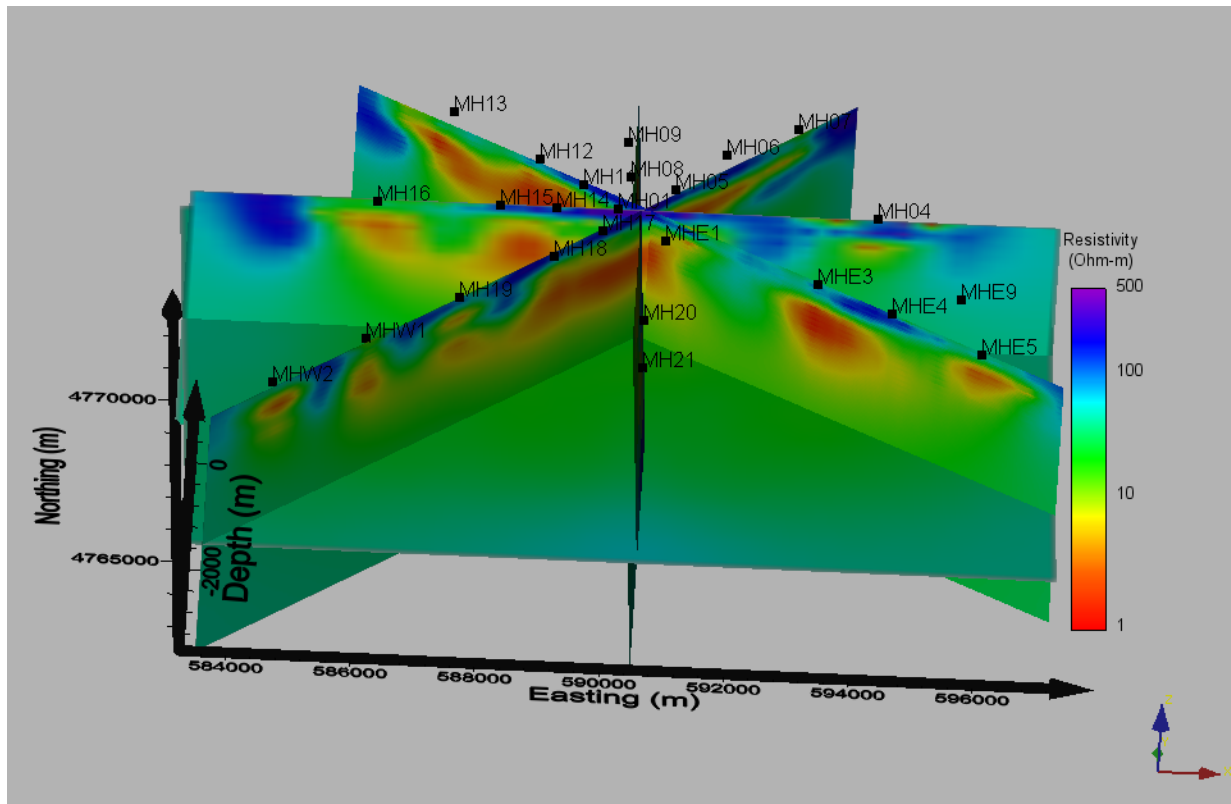
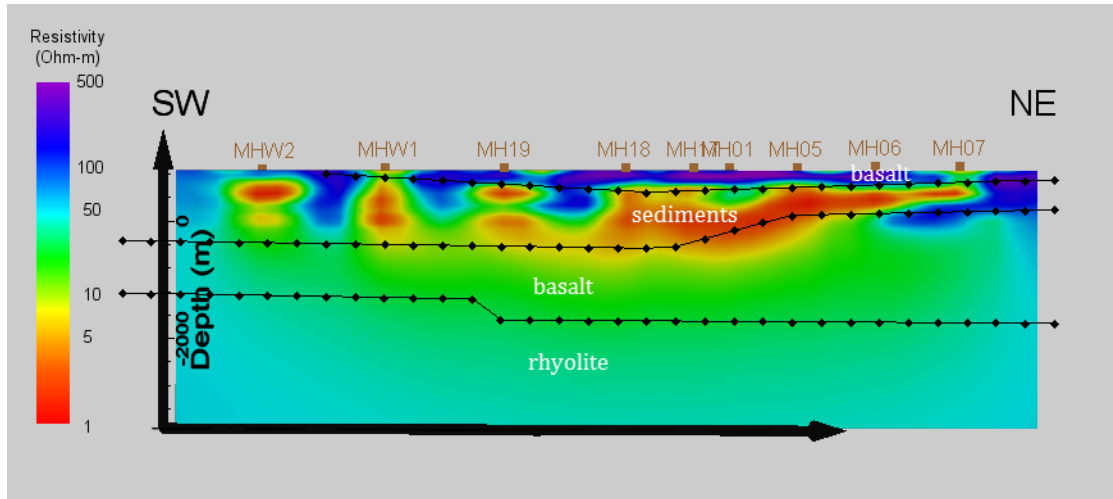


Figure 2a: 3D resistivity model



**Figure 2b:** SW-NE resistivity cross-section extracted from 3D resistivity model. Black lines with diamonds indicate unit interfaces (white labels) from gravity inversion along a profile 3 km SE of this profile.

The above interpretation of MT data forms the basis of the numerical reservoir model presented in the following sections. The latter model differs in the thickness of the permeable zone from the 2-D model of Nielson, et al. (2017). The two models deal with different scales. The model presented in this paper considers a heat source ( $120 \text{ mW/m}^2$ ) emplaced at  $-4500 \text{ mASL}$  over an area of  $500 \text{ km}^2$ . This is consistent with our understanding of the reason for high heat flow on a regional basis--it is associated with sill emplacement at mid-crustal levels. However, the geothermal systems are not ubiquitous in the SRP (and other high heat flow provinces), but only occur locally. Nielson, et al. (2017) considered emplacement of a  $3 \text{ km}^3$  sill at  $1200 \text{ }^\circ\text{C}$  and  $2000 \text{ m}$  depth to explain the observed features of the geothermal system intersected by wells MH-1 and MH-2.

## 2. Computational Volume, Model Grid, and Formation Properties

The ground surface elevation in the Mountain Home area (Figure 1) varies from about  $700 \text{ mASL}$  (meters above sea-level) to  $\sim 1000 \text{ mASL}$ . The MT survey indicates the presence of permeability to a depth of about  $5000 \text{ meters}$  below sea-level (Figure 2b). The bottom of the model grid is placed at  $4500 \text{ m}$  below sea-level; thus the model grid covers essentially all of the permeable volume. The top of the model grid is at the assumed water level (1 bar surface).

In the absence of pressure transient data from any of the wells in the area, the vertical permeability values were determined during the development of the numerical model in order to match the measured well temperatures. The horizontal permeability values in the model are largely unconstrained. In the future, these permeability values will be modified as additional geological, geophysical, and well test data become available.

The model volume is divided into a  $25 \times 20 \times 25$  grid in the x- and y- and z-directions (east, north, and vertically upwards) respectively. In the z-direction, the grid blocks are either  $100 \text{ m}$  or  $250 \text{ m}$ . In the x- and y-directions, a uniform grid spacing of  $1 \text{ km}$  was employed. Indices  $i, j,$  and  $k$  ( $i=1,2, \dots, 25; j=1,2, \dots, 20; k=1, 2, \dots, 25$ ) are used to denote grid block locations in x, y, and z-



directions. The total number of the grid blocks is 12,500, and the model volume is  $2750 \text{ km}^3$  (25 km in the east-west direction, 20 km in the north-south direction, and 5.5 km in the vertical direction). An overlay of the horizontal grid over the Mountain Home area is shown in Figure 3. The vertical grid is displayed in Figure 4. The model area ( $25 \times 20 \text{ km}^2$ ) in Figure 3 is only a small fraction (about 6 %) of the area considered in the regional model (Garg et al., 2016).

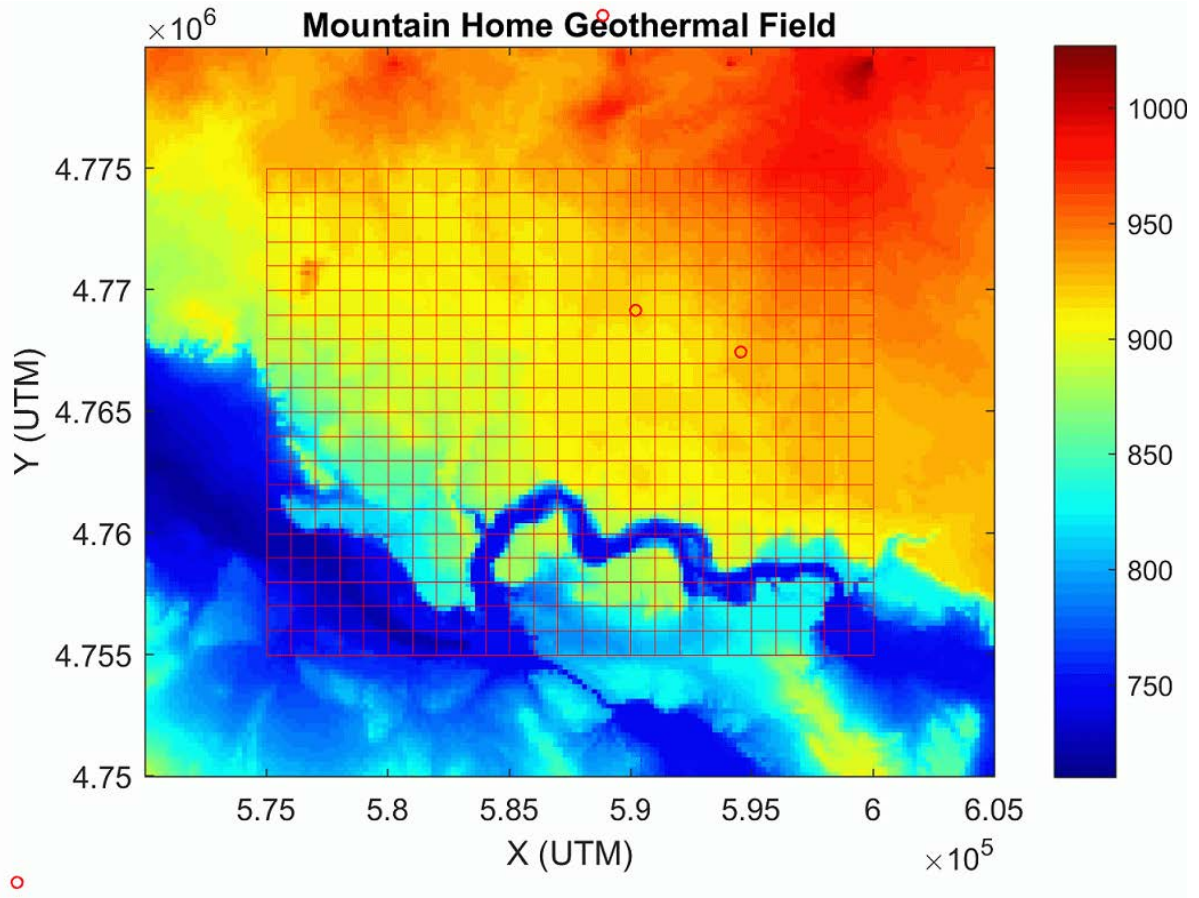


**Figure 3: Horizontal grid (x-y grid) superposed on a topographic map of the Mountain Home area; warm colors denote higher elevations. Well-heads (red circles) are also shown. The origin of the model grid is at 575,000 mE and 4,755,000 mN (UTM).**

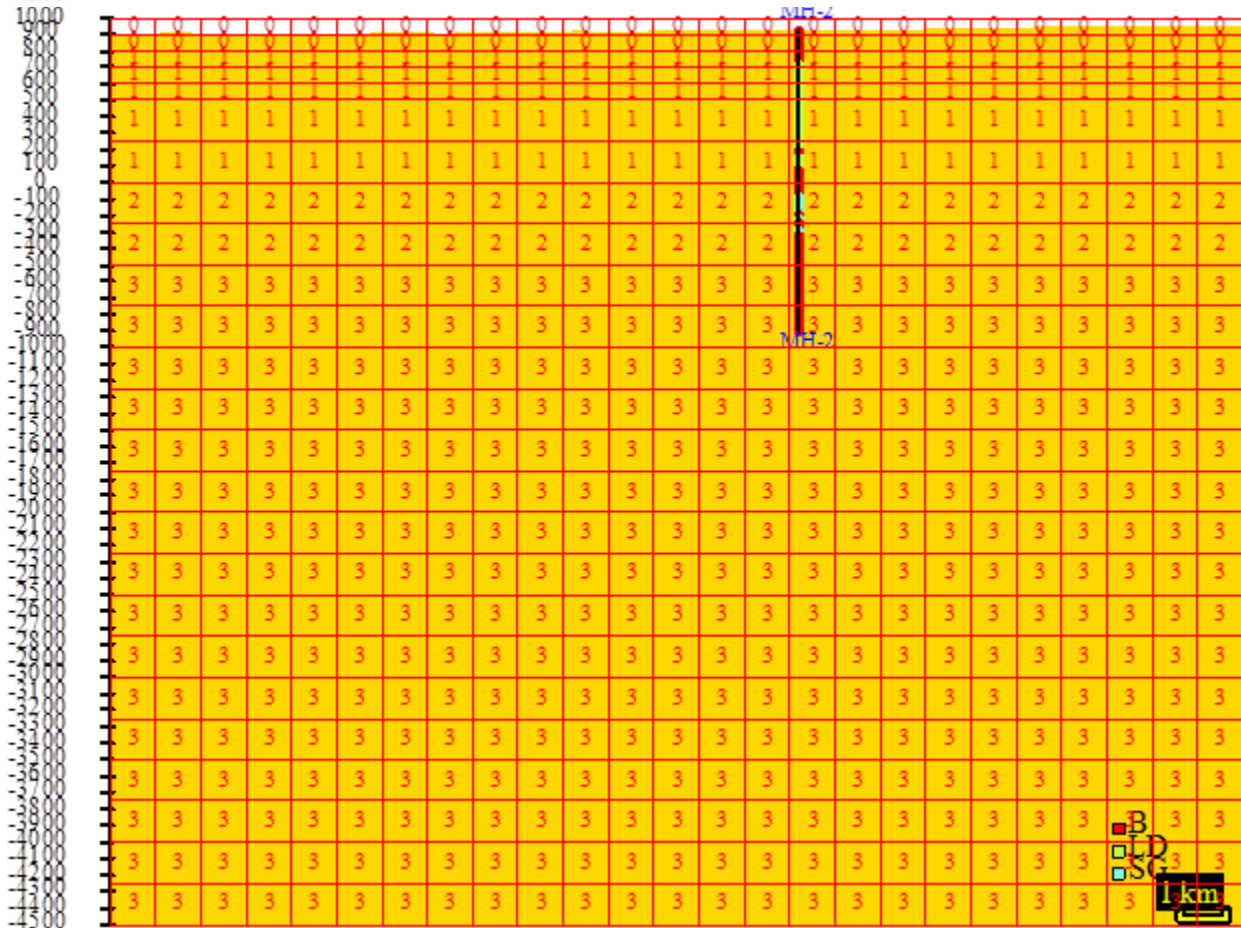


Figure 4: Vertical (x-z) model grid at  $y= 14.5$  km ( $j=15$ ). The bottom of the grid is at  $-4500$  mASL. The bottom 20 grid blocks ( $k=1$  to 20) are of uniform thickness (250 m each); a smaller thickness (100 m) is used for blocks  $k=21$  and higher in order to more closely represent the water level surface. Numbers in grid-blocks (1, 2, 3, and 4) denote the formation type (see below). The void blocks are tagged with 0. Also shown is the lithology from the deep well MH-2 passing through  $j=15$ .

The 3-D numerical model was developed using Leidos’s STAR geothermal reservoir simulator (Pritchett, 2011). To perform model computations, it is essential to prescribe distribution of thermo-hydraulic properties (*e.g.*, permeability, porosity, thermal conductivity, specific heat, etc.) for the entire grid-volume, and boundary conditions along the faces of the model grid. During the development of the natural-state model for the Mountain Home geothermal prospect presented below, the boundary conditions (*i.e.*, heat flux along the bottom boundary, pressure specification along the top boundary) and the formation permeabilities were freely varied in order to match the observed temperature profiles in wells. Several such calculations were carried out; only the final case is described here.

Formation properties utilized for the Mountain Home natural-state model are given in Table 1. Rock types assigned to individual grid blocks are in part based on lithological logs from wells MH-1 and MH-2, and interpretation of gravity and MT surveys. Intrinsic rock density, rock grain specific heat, global thermal conductivity, and porosity values in Table 1 are based on published data (see *e.g.*, Hyndman and Drury, 1977; Eppelbaum et al., 2014; Blackwell, 2013). The average vertical permeability at Mountain Home appears to be rather low. More specifically,

a low vertical permeability is required for matching the mostly conductive temperature profiles recorded in wells MH-1 and MH-2. As mentioned previously, the assumed horizontal permeabilities are essentially arbitrary, and are unconstrained at the present time.

In addition to formation properties given in Table 1, it is necessary to specify capillary pressure and relative permeabilities. The capillary pressure is assumed to be negligible. Straight-line relative permeability curves with a liquid (gas) residual saturation of 0.2 (0.0) are used. Since two-phase flow is unlikely in the “natural state” at Mountain Home, the capillary pressure and relative permeability have no effect on the computed natural-state.

**Table 1: Formation properties.**

Formation Name	Intrinsic rock density (kg/m <sup>3</sup> )	Rock grain specific heat (J/kg-°C)	Global Thermal Conductivity (W/m-°C)	Porosity	Permeability in x-direction (mdarcy)*	Permeability in y-direction (mdarcy)*	Permeability in z-direction (mdarcy)*
1.Sediments/basalt	2800	1000	1.5	0.100	1	1	0.01
2.Basalt upper	2800	1000	1.5	0.025	1	1	0.0135
3.Basalt Lower	2800	1000	1.5	0.025	10	10	1
4.Rhyolite/basalt	2800	1000	1.5	0.025	1	1	0.1

\*It is assumed here that 1 millidarcy is exactly equal to  $10^{-15} \text{ m}^2$

Along the top boundary, the water table (i.e. 1 bar surface) is assumed to be at an elevation given by:

$$z_w = 0.10(z - 720) + 720 = 0.10z + 648 \quad (1)$$

where  $z_w$  denotes the water table elevation (mASL) and  $z$  is the local ground surface elevation.

The ground surface temperature and shallow subsurface temperature gradient are assumed to be  $10^\circ\text{C}$  and  $80^\circ\text{C}/\text{km}$ , respectively. If the water table given by Eq. (1) falls below the mid-point of a grid block, the grid block is flagged as void. Use of Eq. (1) renders all of the grid blocks in layers  $k=24$  and  $k=25$ , and some grid blocks in layer  $k=23$  void. Sources and sinks are imposed in all the top-most grid blocks in each vertical column ( $i, j; i=1, 25$ , and  $j=1, 20$ ) to maintain the pressures and temperatures consistent with Eq. (1), and the assumed surface temperature and shallow subsurface temperature gradient.

Along the bottom boundary, a uniform conductive heat flux ( $120 \text{ mW}/\text{m}^2$ ) is imposed along the entire surface. All the vertical faces of the grid are assumed to be impermeable and insulated. The reservoir fluid is treated as pure water.

### 3. Computation of Natural State

Starting from an essentially arbitrary cold state, the computation was marched forward in time for about 625,000 years. The maximum time step used was 25 years. The change in total thermal energy in the computational grid is displayed in Figure 5. For most of the computational period, the thermal energy continues to increase and the fluid mass declines. Initially the change is rapid; it moderates over time. After about 500,000 years, the change is quite small over a time scale of 50 to 100 years. The computed temperature values at cycle 25,000 (about 625,000 years) were compared with the available data.

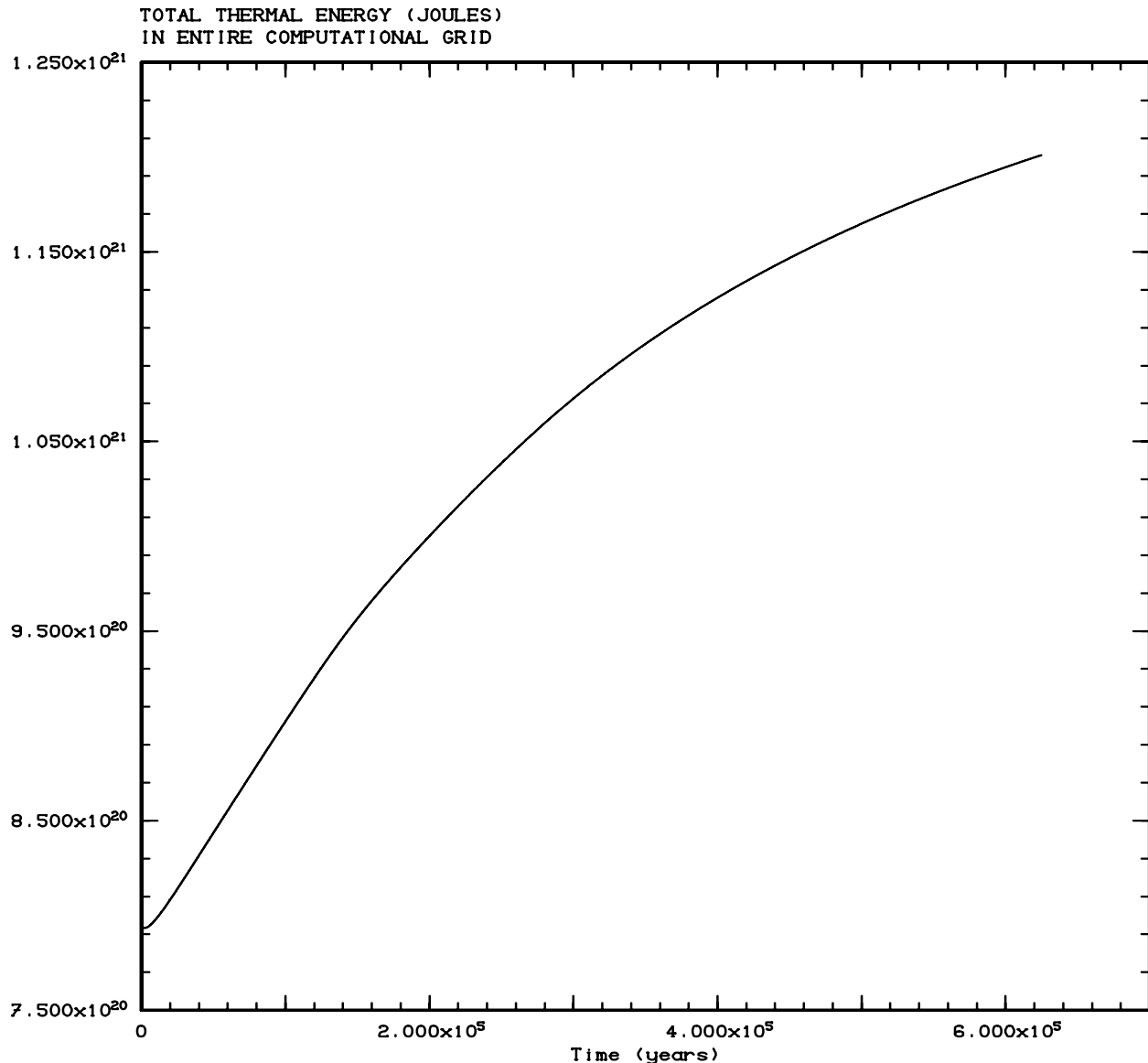
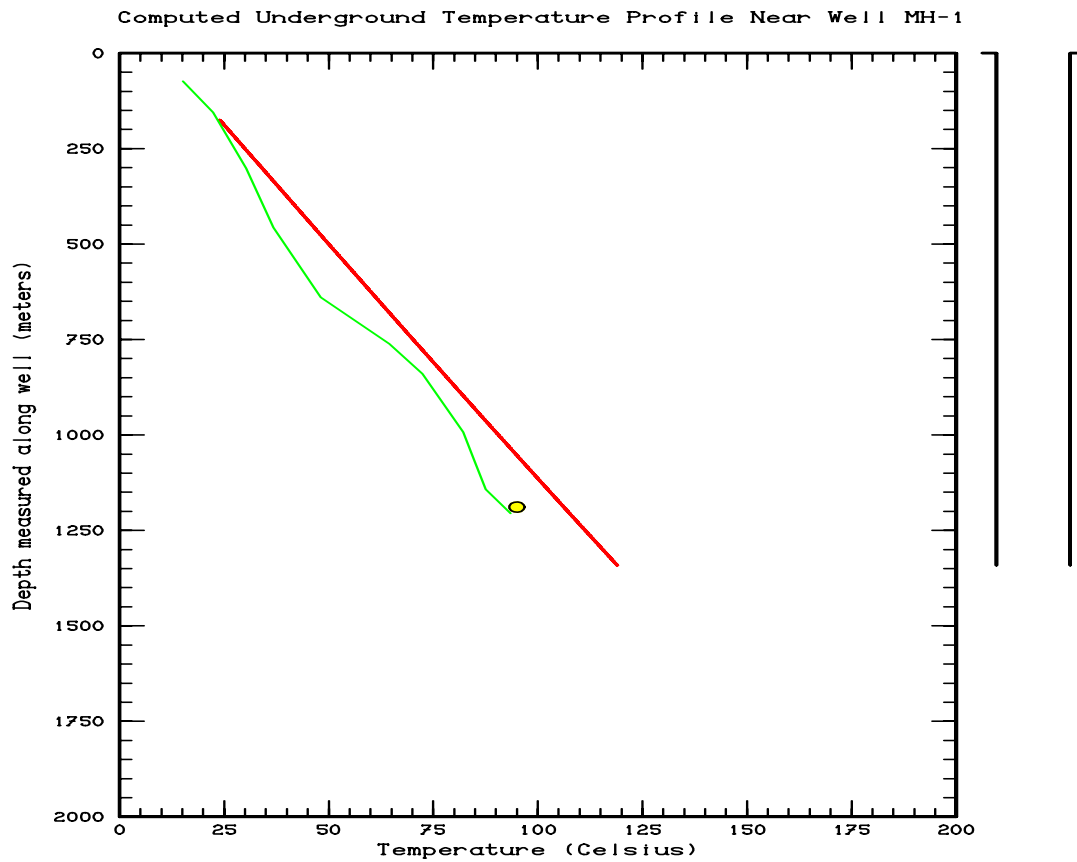


Figure 5: Computed total thermal energy in the computational grid.

The measured temperatures in Mountain Home wells MH-1 and MH-2 (Nielson and Shervais, 2014) are compared with calculated results from the model in Figures 6 and 7. It is not known if the available temperature data represent stable formation temperatures. No information on shut-



in time is available regarding the temperature surveys for well MH-1. Given the current data limitations, the agreement between the measured and computed temperature values is considered satisfactory.



**Figure 6: Comparison between computed (solid red line) and measured temperature profiles (solid green line and yellow circle) for well MH-1. No information is available concerning the shut-in time at which the temperature survey was taken.**

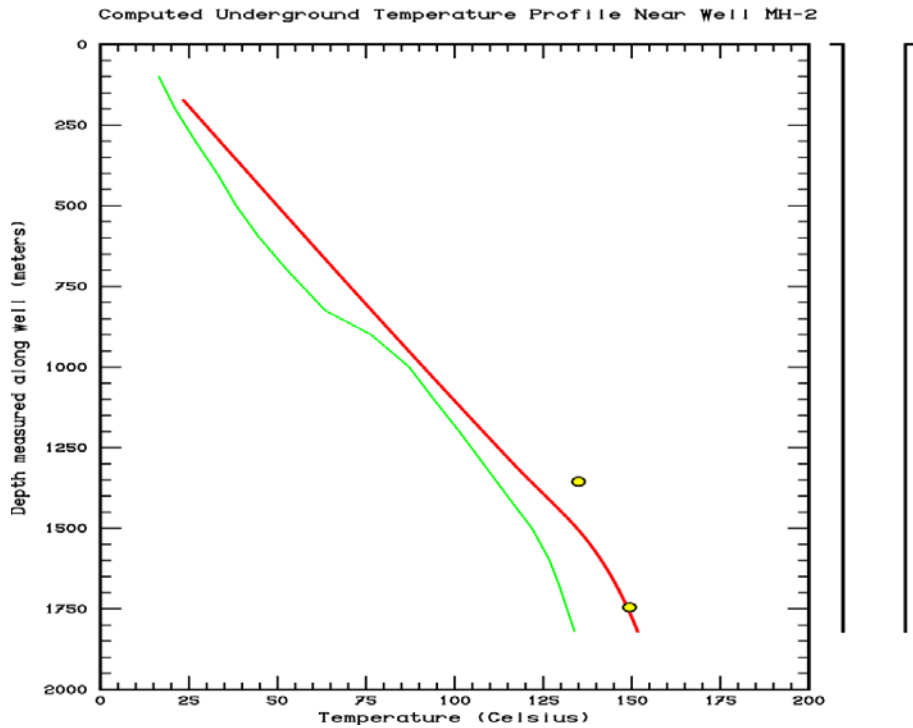


Figure 7: Comparison between computed (solid red line) and measured temperature profiles (solid green line) for well MH-2. The yellow circles are the measured flowing temperatures. Since the measured flowing temperatures are higher than the recorded shut-in temperatures (solid green line), it is almost certain that the shut-in survey does not represent the stable formation temperatures.

#### 4. Computed Temperature Distribution and Fluid Flow

Computed temperatures and fluid flux vectors in three vertical x-z ( $j=4, 15, 19$ ), and one horizontal x-y ( $k=14$ ) planes are exhibited in Figures 8 and 9, respectively. Two of the vertical planes ( $j=4$  and  $19$ ) are located in areas with either small reservoir thickness or low reservoir permeability; little or no convective flow is seen along these planes. Vertical plane  $j=15$  passes close to well MH-2, and contains a relatively thick permeable layer; convective flow extends to shallow depths (about 1000 to 1500 m) along this plane. Significant fluid flow is restricted to permeable basalt layer. Isotherms in Figures 9 exhibit the existence of at least three convective cells in the northern portion of the grid; note that this area is north of the deep gravity fault (Figure 1), and very likely contains a permeable reservoir below the shallow sediments.

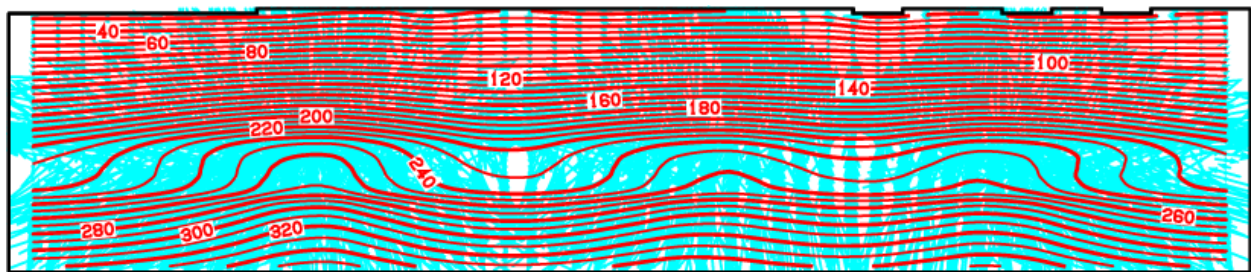


Figure 8a: Isotherms (red lines) and flow vectors (blue) in the vertical x-z plane  $j=4$ .

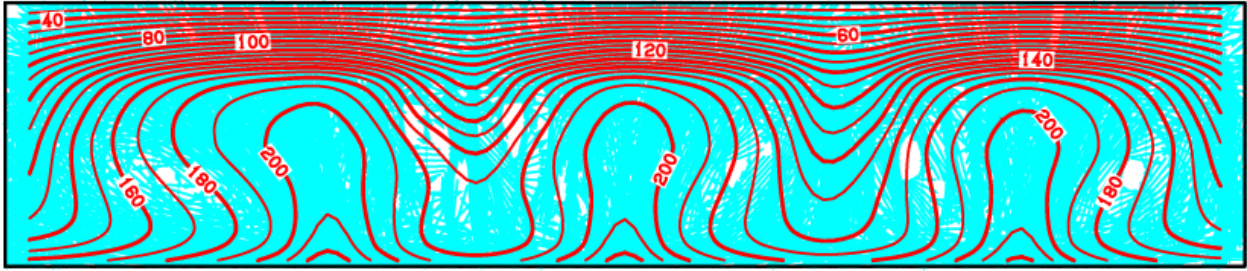


Figure 8b: Isotherms (red lines) and flow vectors (blue) in the vertical x-z plane  $j=15$ .

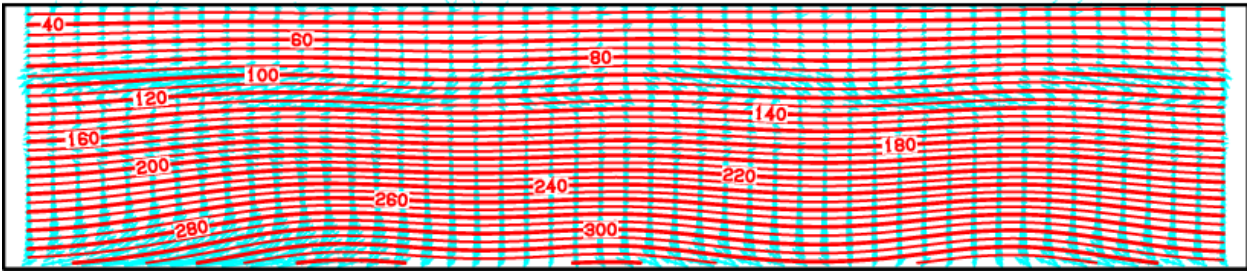


Figure 8c: Isotherms (red lines) and flow vectors (blue) in the vertical x-z plane  $j=19$ .

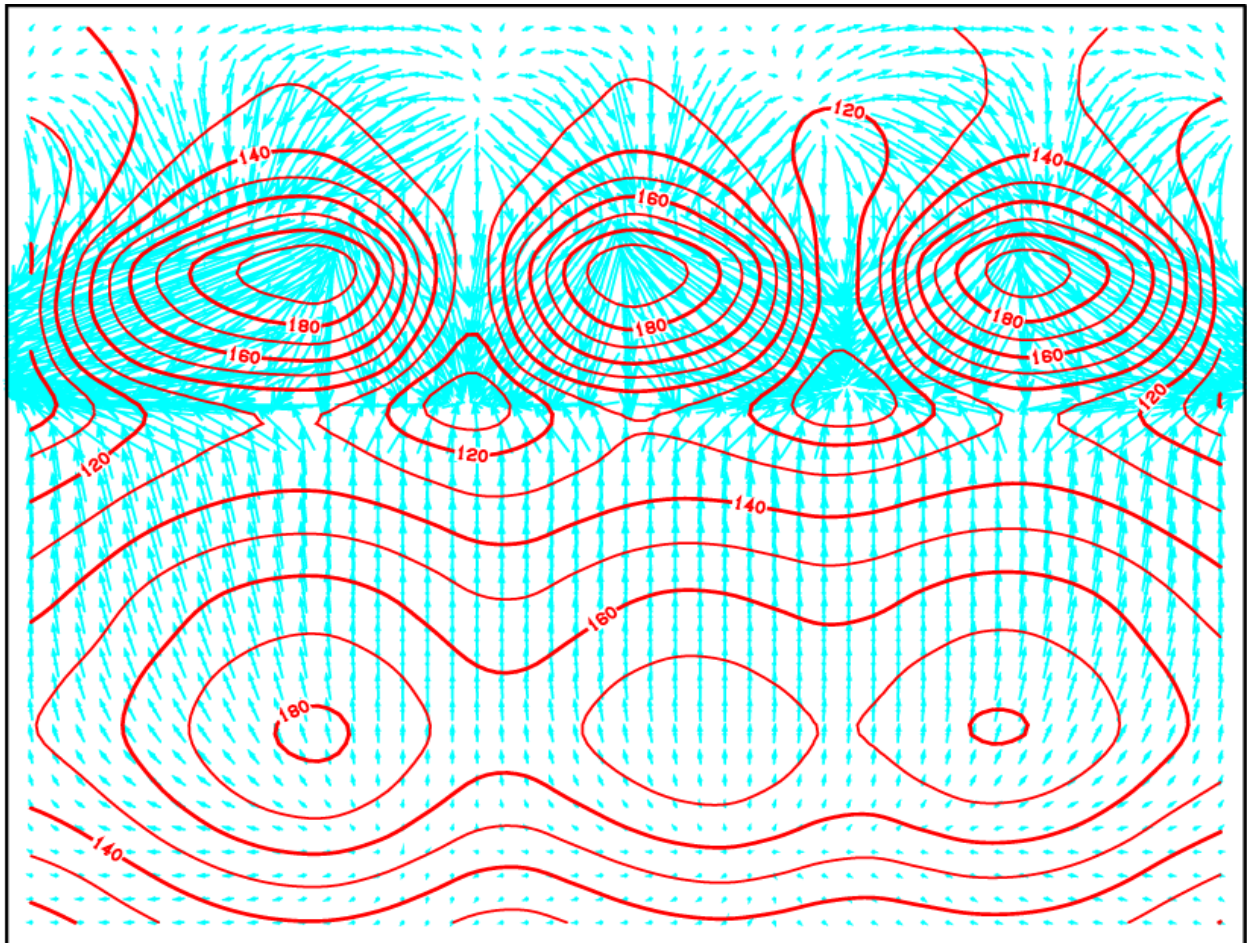


Figure 9: Isotherms (red lines) and flow vectors (blue) in the horizontal x-y plane  $k=14$ .

## 5. Concluding Remarks

The preceding sections present a 3-D natural state model for the Mountain Home geothermal prospect. The latter model covers only a small part (about 6 %) of the area included in the regional model (Garg, 2016). The regional model was conditioned using the available temperature data from five deep wells in the area, and incorporated a particularly simple representation of lithology. Since the regional model was developed, various geophysical surveys (gravity, magnetic, MT) surveys have been carried out in the area. Results from the gravity and MT surveys have provided important information that enabled to estimate permeability distribution in the Mountain Home area. The current natural state model incorporates the latter information, and therefore provides a more accurate representation of the subsurface. At present, no pressure or reservoir permeability data are available. Acquisition of pressure data will require access to deep wells; such access is also required for well tests designed to measure subsurface permeability distribution. Current plans call for the drilling and testing of a well in the next phase of the Snake River Plain Fairway Project. The reservoir model will be updated as these additional data become available.

### *Acknowledgment*

*This paper was supported in part by the U. S. Department of Energy, Geothermal Technologies Office through award DE-EE0006733 to Utah State University. This work was also supported with funding by the office of the Assistant Secretary for Energy Efficiency and Renewable Energy, Geothermal Technologies Office, of the U.S. Department under the U.S. Department of Energy Contract No. DE-AC02-05CH11231 with Lawrence Berkeley National Laboratory.*

## REFERENCES

- Blackwell, D. "SMU Geothermal Laboratory heat flow database." Available through National Geothermal Data System (2013).
- Eppelbaum, L., Kutasov, I., and Pilchin, A. "Applied Geothermics." Springer, (2014), 99-149.
- Garg, S.K. "Thermal modeling of the Mountain Home Geothermal Area." *Proceedings: 41st Workshop on Geothermal Reservoir Engineering*, Stanford University, Stanford, CA (2016).
- Glen, J.M.G., Liberty, L., Gasperikova, E., Siler, D., Shervais, J., Ritzinger, B., Athens, N., and Earney, T. "Geophysical Investigations and Structural Framework of Geothermal Systems in west and southcentral Idaho: Camas Prairie and Mountain Home." *Proceedings: 42nd Workshop on Geothermal Reservoir Engineering*, Stanford University, Stanford, CA (2017).
- Hyndman, R.D., and Drury, M.J. "Physical properties of basalts, gabbros and ultramafic rocks from DSDP Leg 37." *Initial Reports DSDP*, (1977), 395-401.
- Nielson, D.L, and Shervais, J.W. "Conceptual Model for Snake River Plain Geothermal System." *Proceedings: 39th Workshop on Geothermal Reservoir Engineering*, Stanford University, Stanford, CA (2014).

Nielson, D.L, Sonnenthal, E., Shervais, J.W., and Garg, S.K. “Mafic Heat Sources for Snake River Plain Geothermal Systems.” *Proceedings: 42nd Workshop on Geothermal Reservoir Engineering*, Stanford University, Stanford, CA (2017).

Pritchett, J.W. “STAR User’s Manual Version 11.0.” Leidos Inc., San Diego, CA (2011).

Shervais, J.W., Glen, J.M., Nielson, D., Garg, S., Dobson, P., Gasperikova, E., Sonnenthal, E., Visser, C., Liberty, J.M., Deangelo, J., Siler, D., and Evans, J.P. “Play Fairway Analysis of the Snake River Plain: Phase 1.” *Proceedings: 41st Workshop on Geothermal Reservoir Engineering*, Stanford University, Stanford, CA (2016).

Shervais, J.W., Glen, J.M., Nielson, D., Garg, S., Liberty, L.M., Siler, S., Dobson, P., Gasperikova, E., Sonnenthal, E., Neupane, G., DeAngelo, J., Evans, J.P., Snyder, N., and Newell, D.L. “Geothermal Play Fairway Analysis of the Snake River Plain: Phase 2.” *Geothermal Resources Council Transactions 41* (2017).